*Electronic Supplementary Information*

# Thiophene-Based Dyes for Probing Membranes

Ismael López-Duarte,[a] Phoom Chairatana,[a] Yilei Wu,[b] Javier Pérez-Moreno,[c] Philip M. Bennett,[a] James E. Reeve,[a] Igor Boczarow,[a] Wojciech Kaluza,[a] Neveen A. Hosny,[b] Samuel D. Stranks,[d] Robin J. Nicholas,[d] Koen Clays,*[c] Marina K. Kuimova*[b] and Harry L. Anderson*[a]

**Table of Contents** **page**

1) Synthesis and compound characterization S2
2) Spectroscopic properties S4
    Fig. S1 $^{1}$H NMR spectrum of **1a** S4
    Fig. S2 $^{13}$C NMR spectrum of **1a** S4
    Fig. S3 $^{1}$H NMR spectrum of **1b** S5
    Fig. S4 $^{13}$C NMR spectrum of **1b** S5
    Fig. S5 $^{1}$H NMR spectrum of **2a** S6
    Fig. S6 $^{13}$C NMR spectrum of **2a** S6
    Fig. S7 $^{1}$H NMR spectrum of **2b** S7
    Fig. S8 $^{13}$C NMR spectrum of **2a** S7
    Table S1 Photophysical properties of the **FM4-64**, **1b** and **2b** S8
    Fig. S9 Normalized absorption and emission spectra of **2b**, **1a** and **2a** S9
    Fig. S10 Solvatochromic properties of **FM4-64**, **1b** and **2b** S9
    Fig. S11 Fluorescence spectra of **FM4-64** and **1b** in water and micelles S10
3) Hyper-Rayleigh Scattering S10
4) Dark Toxicity and Phototoxicity Experimental Procedures S11
5) Dark Toxicity Data S12
6) Phototoxicity Data S14
7) Fluorescence Imaging S16
    Fig. S12 Direct fluorescent intensity comparison between **FM4-64** and **1b** in live cells S16
    Fig. S13 Time-dependent cell uptake of **FM4-64**, **1b** and **2b** monitored by fluorescence S17
    Fig. S14 Two-photon fluorescence and SHG images of HeLa cells incubated with **2b** S17
8) Voltage-sensitivity data analysis S17
    Table S2 Relative sensitivities of **FM4-64**, **1b** and **2b** S18
    Fig. S15 Voltage-dependent SHG and TPEF traces of **FM4-64** S18
    Fig. S16 Voltage-dependent SHG and TPEF traces of **1b** S18
    Fig. S17 Voltage-dependent SHG and TPEF traces of **2b** S19
    Fig. S18 Change in SHG and TPEF intensity against applied potential of **FM4-64** and **1b** S19
9) References S20

[a] *Department of Chemistry, Oxford University, Chemistry Research Laboratory, Oxford, UK OX1 3TA.*
*E-mail: harry.anderson@chem.ox.ac.uk*

[b] *Chemistry Department, Imperial College London, Exhibition Road, London, UK SW7 2AZ.*
*E-mail: m.kuimova@imperial.ac.uk*

[c] *Department of Chemistry, University of Leuven, Celestijnenlaan 200 D, 3001 Leuven, Belgium.*
*E-mail: koen.clays@fys.kuleuven.be*

[d] *Department of Physics, Oxford University, Clarendon Laboratory, Oxford, UK OX1 3PU.*

# 1) Synthesis and Compound Characterization

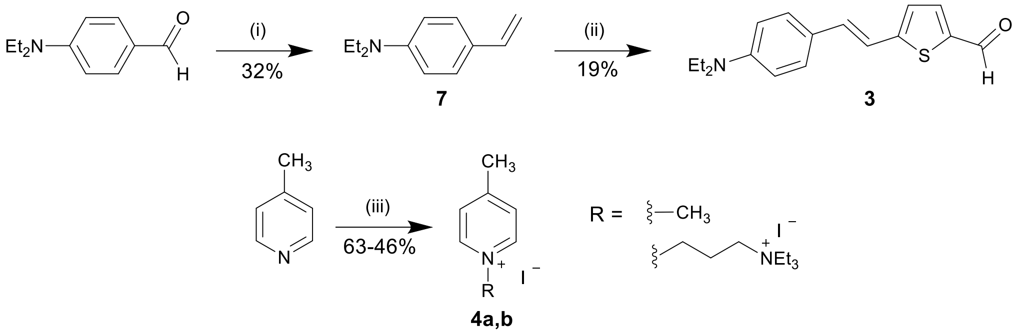

**Scheme 1.** Synthesis of derivatives **3** and **4a,b**: (i) $MePh_3PBr$, *n*-BuLi, THF; (ii) 5-Bromothiophene-2-carbaldehyde, $Pd(OAc)_2$, *n*-$Bu_3N$, 120 °C, 24 h; (iii) MeI, $Et_2O$, 20 °C, 3 h or (3-iodopropyl)triethylammonium iodide, DMF, 100 °C, 48 h.

### *N,N*-Diethylaminostyrene (7)[1]

To a stirred slurry of methyltriphosphonium bromide (11.1 g, 31.0 mmol) in dry THF (50 mL) under argon atmosphere and cooled to 0 °C was added *n*-butyl lithium (27.5 mL, 44.0 mmol, 1.6 M in hexanes) via syringe. The solution was stirred in an ice bath for another 15 min, then a solution of 4-(*N,N*-diethylamino)benzaldehyde (5.00 g, 28.2 mmol) in dry THF (20 mL) was rapidly added with stirring by means of an addition funnel. The turbid mixture was stirred in an ice bath for another 20 min then allowed to warm to room temperature overnight in the dark. The mixture was then cooled in an ice bath and quenched by the dropwise addition of water (80 mL). The aqueous mixture was extracted twice with $Et_2O$. The combined ether extracts were washed twice with saturated brine, dried over $MgSO_4$, and concentrated to dryness. The crude product was purified by column chromatography ($SiO_2$, 5% EtOAc in PET 40–60° with 1% triethylamine). The product **7** was obtained as a colorless oil. Yield 1.56 g (32%). $^1$H NMR (400 MHz, $CDCl_3$) $\delta_H$ 1.17 (t, $J$ = 7.1 Hz, 6H), 3.37 (q, $J$ = 7.1 Hz, 4H), 4.99 (dd, $J$ = 10.9 Hz, $J$ = 0.97 Hz, 1H), 5.52 (dd, $J$ = 17.5 Hz, $J$ = 0.97 Hz, 1H), 6.63 (dd, $J$ = 17.5 Hz, $J$ = 10.8 Hz, 1H), 6.64 (d, $J$ = 8.9 Hz, 2H), 7.29 (d, $J$ = 8.8 Hz, 2H); $^{13}$C NMR (100 MHz, $CDCl_3$) $\delta_C$ 12.64, 44.41, 108.66, 111.57, 125.15, 127.42, 136.68, 147.50; MS (ESI) *m/z* 176.14 ($C_{12}H_{18}N$, $[M+H]^+$, requires 176.14, 100%).

### 5-{(*E*)-2-[4-(Diethylamino)phenyl]ethenyl}thiophene-2-carboxaldehyde (3)[2]

To a Schlenk tube were added *N,N*-diethylaminostyrene **1** (1.56 g, 8.91 mmol), 5-bromo-2-thiophene carboxaldehyde (1.27 mL, 10.7 mmol), palladium(II) acetate (30.0 mg, 89.0 µmol), tris-(*o*-tolyl)phosphine (54.3 mg, 178 µmol) and tributylamine (4 mL). The mixture was degassed by three freeze-thaw cycle before purging with nitrogen and then stirred at 115 °C for 22 h. The resulting red mixture was cooled, then partitioned between $CH_2Cl_2$ (50 mL) and water (50 mL). The aqueous layer was washed with $CH_2Cl_2$ (2 × 40 mL). The organic layers were combined, dried over $MgSO_4$ and the solvents were removed by rotary evaporation. The crude product was purified by a short column chromatography ($SiO_2$, 5% EtOAc in hexane) to give **3** as a bright orange solid. Yield 489 mg (19%). m.p. 136–138 °C; $^1$H NMR (400 MHz, $CDCl_3$) $\delta_H$ 1.20 (t, $J$ = 7.0 Hz, 6H), 3.41 (q, $J$ = 7.0 Hz, 4H), 6.66 (d, $J$ = 8.9 Hz, 2H), 6.96 (d, $J$ = 16.0 Hz, 1H), 7.05 (d, $J$ = 3.9 Hz, 1H), 7.10 (d, $J$ = 16.0 Hz, 1H), 7.38 (d, $J$ = 8.9 Hz, 2H), 7.63 (d, $J$ = 3.9 Hz, 1H), 9.82 (s, 1H, CHO); $^{13}$C NMR (100 MHz, $CDCl_3$) $\delta_C$ 12.63, 44.42, 111.50, 115.53, 122.91, 124.79, 128.64, 133.69, 137.63, 139.99, 148.28, 154.51, 182.29; MS (ESI) *m/z* 286.15 ($C_{17}H_{20}NOS$, $[M+H]^+$, requires 286.13, 100%), 308.14 ($C_{17}H_{19}NNaOS$, $[M+Na]^+$, requires 308.11, 30%).

### 1,4-Dimethylpyridin-1-ium iodide (4a)[3]

4-Methylpyridine (1.05 mL, 10.7 mmol), methyl iodide (1.32 mL, 21.1 mmol) and anhydrous $Et_2O$ (3 mL) were stirred at room temperature for 3 h. The product precipitated out during the reaction. The product was filtered out and washed with $Et_2O$, to give **4a** as pale yellow solid. Yield 1.58 g (63%). m.p. 148–150 °C; $^1$H NMR (400 MHz, $CD_3OD$) $\delta_H$ 2.69 (s, 3H), 4.37 (s, 3H), 7.95 (d, $J$ = 5.9 Hz, 2H), 8.77 (d, $J$ = 5.9 Hz, 2H); $^{13}$C NMR (125 MHz, $CD_3OD$) $\delta_C$ 9.39, 22.02, 129.70, 145.80, 160.87; MS (ESI) *m/z* 108.08 ($C_7H_{10}IN$, $M^+$, requires 108.08, 100%).

### 4-Methyl-1-[3-(triethylammonio)propyl]pyridin-1-ium iodide (4b)[4]

4-Methylpyridine (0.59 mL, 5.54 mmol), (3-iodopropyl)triethylammonium iodide (2.00 g, 5.04 mmol) and dry DMF (4 mL) were stirred at 100 °C for 48 h. After cooling, the precipitates were filtered out and washed with $CH_2Cl_2$ to give **5** as a pale pink solid. Yield 1.12 g (46%). m.p. 210–212 °C; $^1$H NMR (400 MHz, $CD_3OD$) $\delta_H$ 1.36 (t, $J$ = 7.2 Hz, 9H), 2.50–2.61 (m, 2H), 2.72 (s, 3H), 3.43 (q, $J$ = 7.2 Hz, 6H), 3.49 (m, 2H), 4.79 (t, $J$ = 7.9 Hz, 2H), 8.00 (d, $J$ = 6.5 Hz, 2H), 9.04 (d, $J$ = 6.5 Hz, 2H); $^{13}$C NMR (100 MHz, $CD_3OD$) $\delta_C$ 8.0, 22.1, 25.2, 54.4, 54.5, 58.3, 130.1, 145.2, 161.9; MS (ESI) *m/z* 235.22 ($C_{15}H_{27}N_2$, $[M-H]^+$, requires 235.22, 100%).

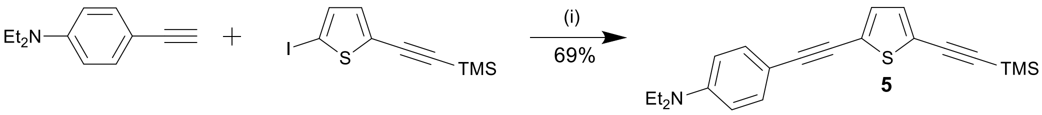

**Scheme 2.** Synthesis of derivative **5**: (i) $Pd(PPh_3)_2Cl_2$, $PPh_3$, CuI, toluene, *i*-$Pr_2NH$, 20 °C, 2 h.

### *N,N*-Diethyl-4-({5-[(trimethylsilyl)ethynyl]thiophen-2-yl}ethynyl)aniline (5)[5]

In a Schlenk tube, *N,N*-diethyl-4-ethynylaniline (341 mg, 1.97 mmol) was dissolved in a mixture of dry toluene (5 mL) and distilled diisopropylamine (5 mL) and the solution was degassed by three freeze-thaw cycles before purging with nitrogen. ((5-Iodothiophen-2-yl)ethynyl) trimethylsilane (723 mg, 2.36 mmol), bis(triphenylphosphine) palladium(II) chloride (69.0 mg, 98.4 μmol) and copper(I) iodide (37.5 mg, 197 μmol) were then added to the solution (the two catalysts were dried *in vacuo* for 30 min immediately before use). The reaction mixture was then flushed with nitrogen and stirred at room temperature for 2 h. The mixture was then diluted with $CH_2Cl_2$ (50 mL) and washed with distilled water (50 mL), saturated aqueous $NH_4Cl$ (50 mL) and distilled water (50 mL). The organic layer was dried over anhydrous $MgSO_4$ and the solvents were removed by rotary evaporation. The crude product was further purified by column chromatography ($SiO_2$, a gradient of $CHCl_3$ in PET 40–60 °). The product **5** was obtained as a white solid. Yield 475 mg (69%). m.p. 140–142 °C; $^1$H NMR (400 MHz, $CDCl_3$) $\delta_H$ 0.26 (s, 9H, $SiMe_3$), 1.19 (t, $J$ = 7.1 Hz, 6H), 3.38 (q, $J$ = 7.1 Hz, 4H), 6.61 (d, $J$ = 9.0 Hz, 2H), 7.01 (d, $J$ = 3.7 Hz, 1H), 7.09 (d, $J$ = 3.7 Hz, 1H), 7.36 (d, $J$ = 9.0 Hz, 2H); $^{13}$C NMR (100 MHz, $CDCl_3$) $\delta_C$ -0.16, 12.54, 44.34, 80.02, 95.65, 97.34, 99.40, 107.87, 111.11, 123.07, 126.11, 130.28, 132.58, 132.95, 147.82; MS (ESI) *m/z* 352.19 ($C_{21}H_{26}NSSi$, $[M+H]^+$, requires 352.16, 100%).

## 2) Spectroscopic Data

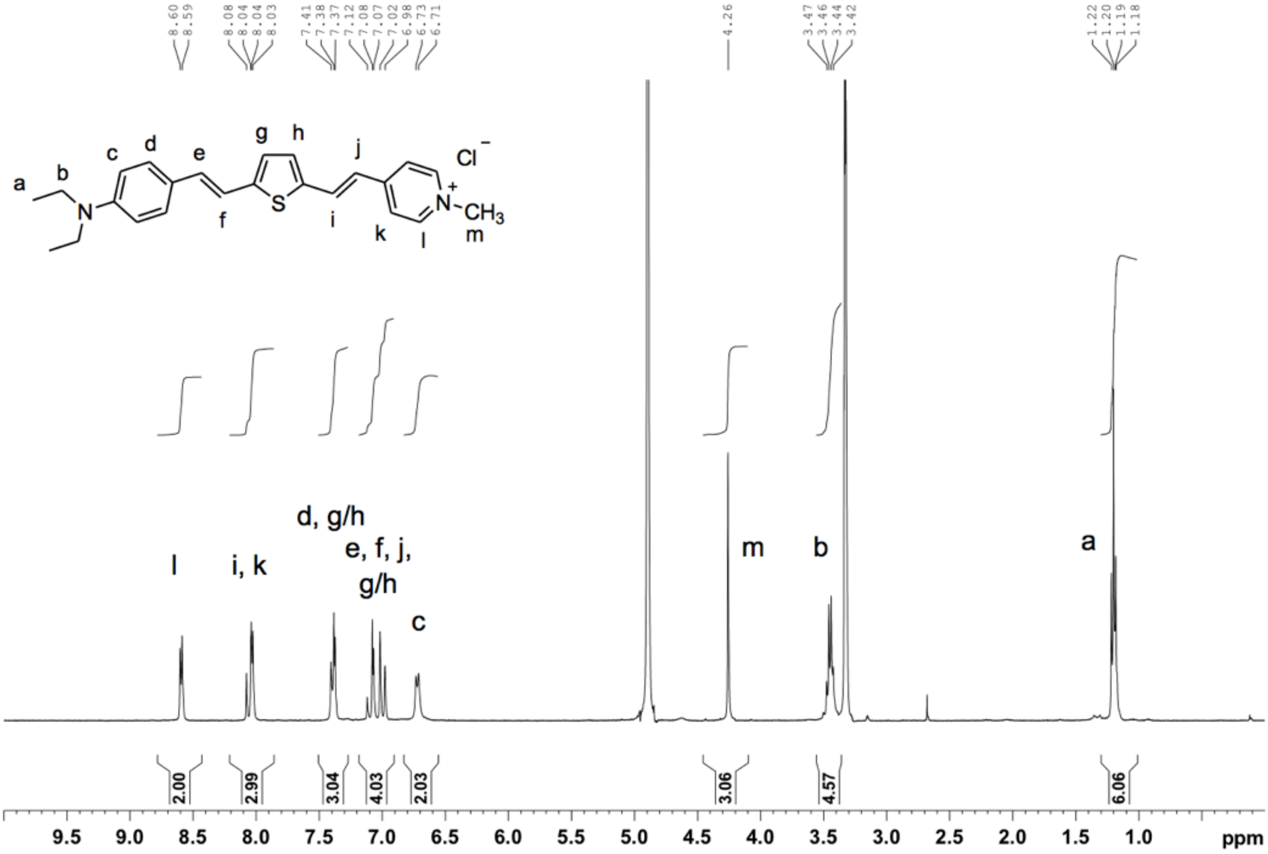

**Fig. S1.** $^1$H NMR spectrum of **1a** (400 MHz, $CD_3OD$).

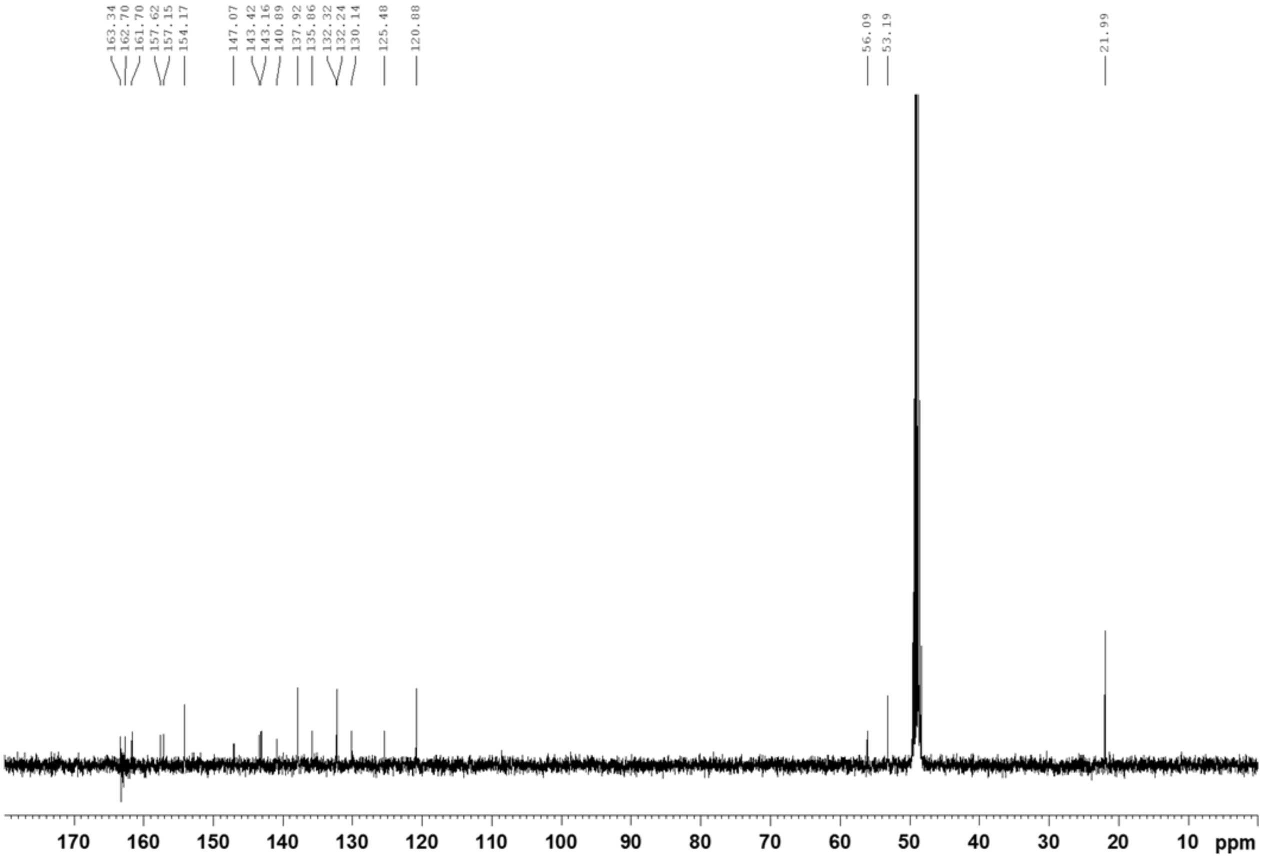

**Fig. S2.** $^{13}$C NMR spectrum of **1a** (100 MHz, $CD_3OD$).

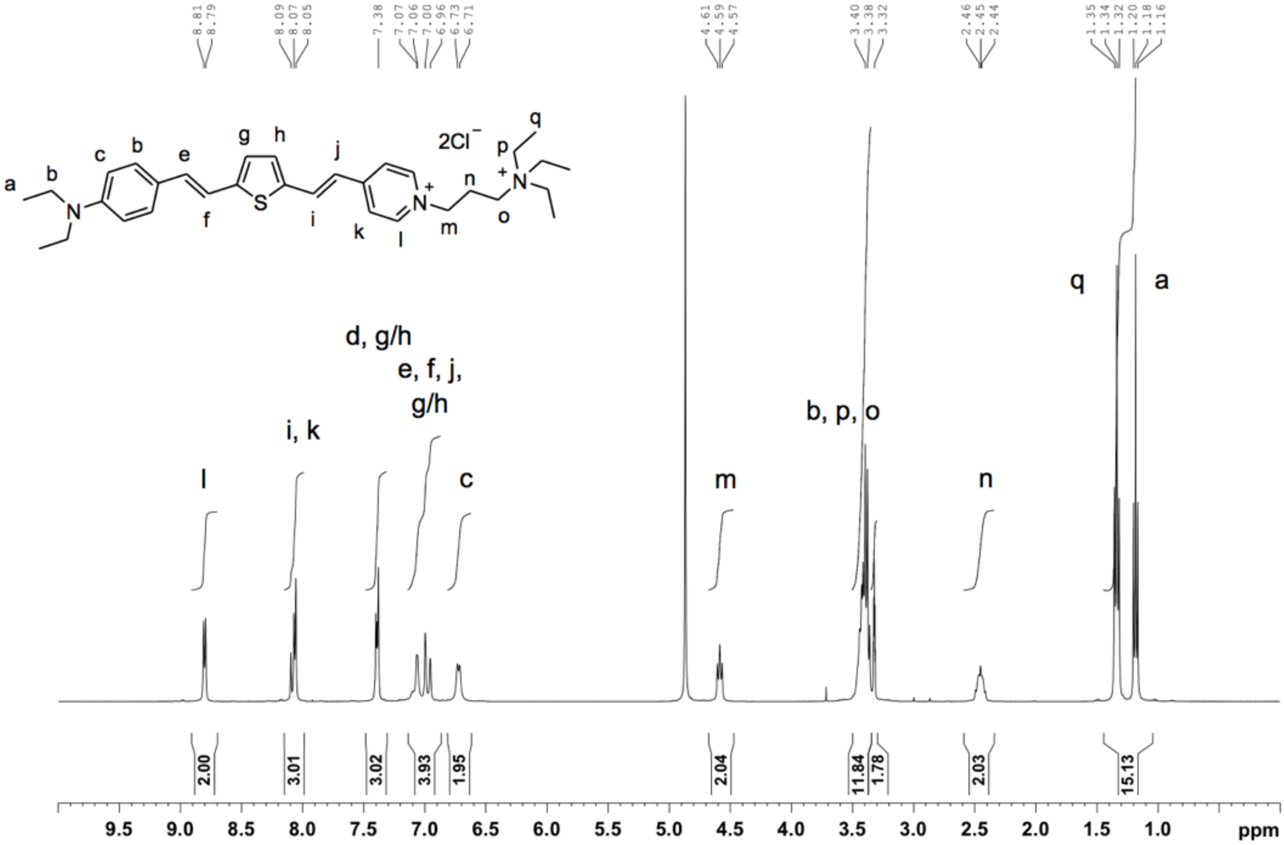

**Fig. S3.** $^1$H NMR spectrum of **1b** (400 MHz, $CD_3OD$).

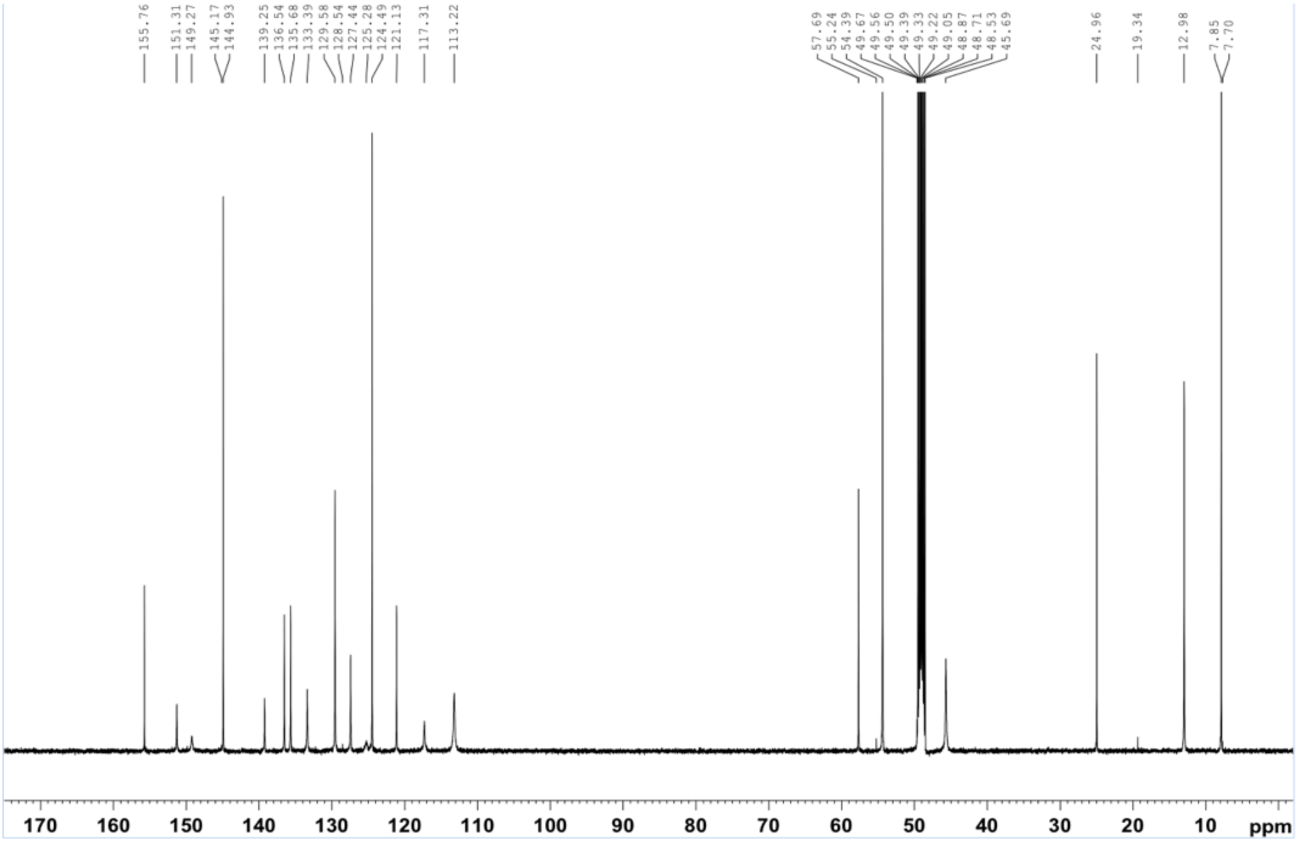

**Fig. S4.** $^{13}$C NMR spectrum of **1b** (125 MHz, $CD_3OD$).

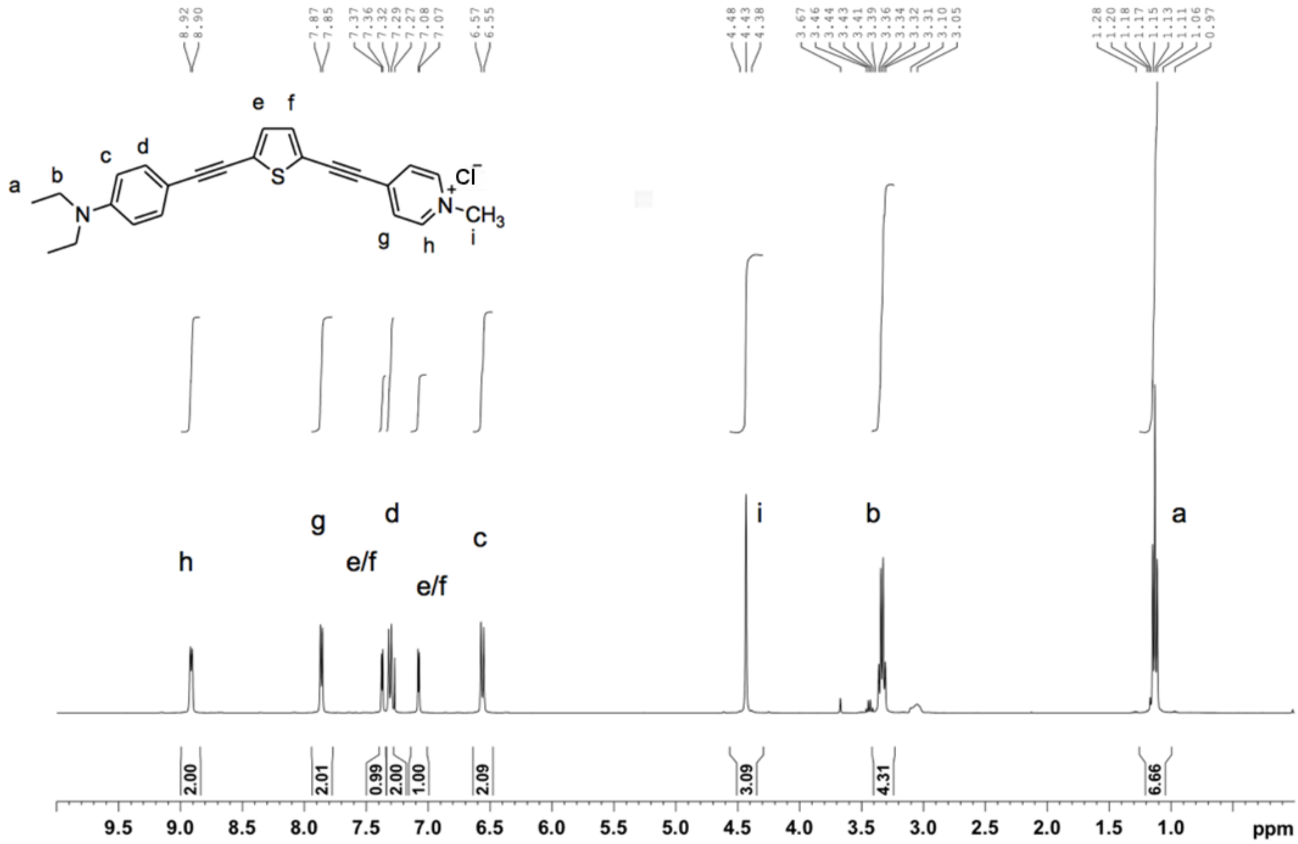

**Fig. S5.** $^1$H NMR spectrum of **2a** (400 MHz, $CDCl_3$).

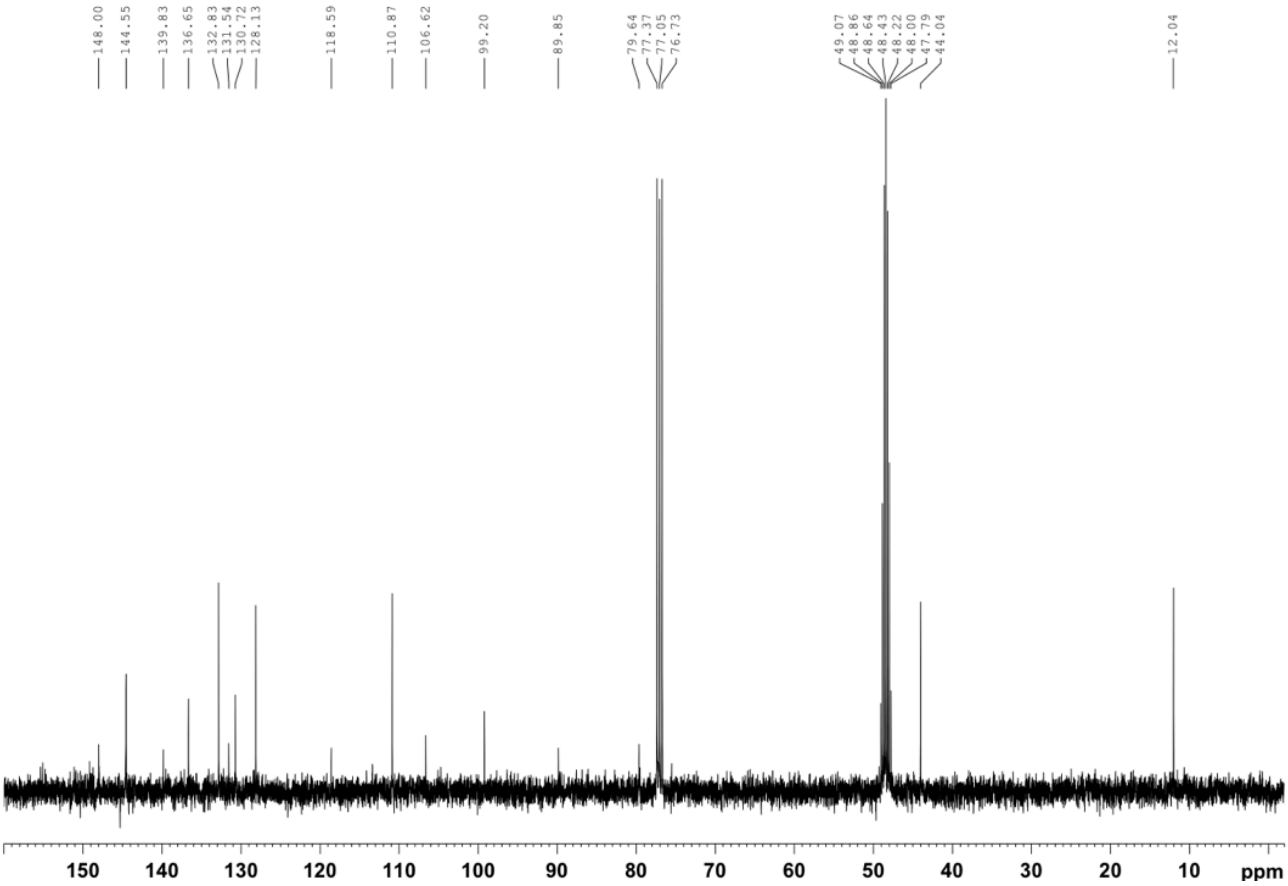

**Fig. S6.** $^{13}$C NMR spectrum of **2a** (100 MHz, $CDCl_3$ + $CD_3OD$).

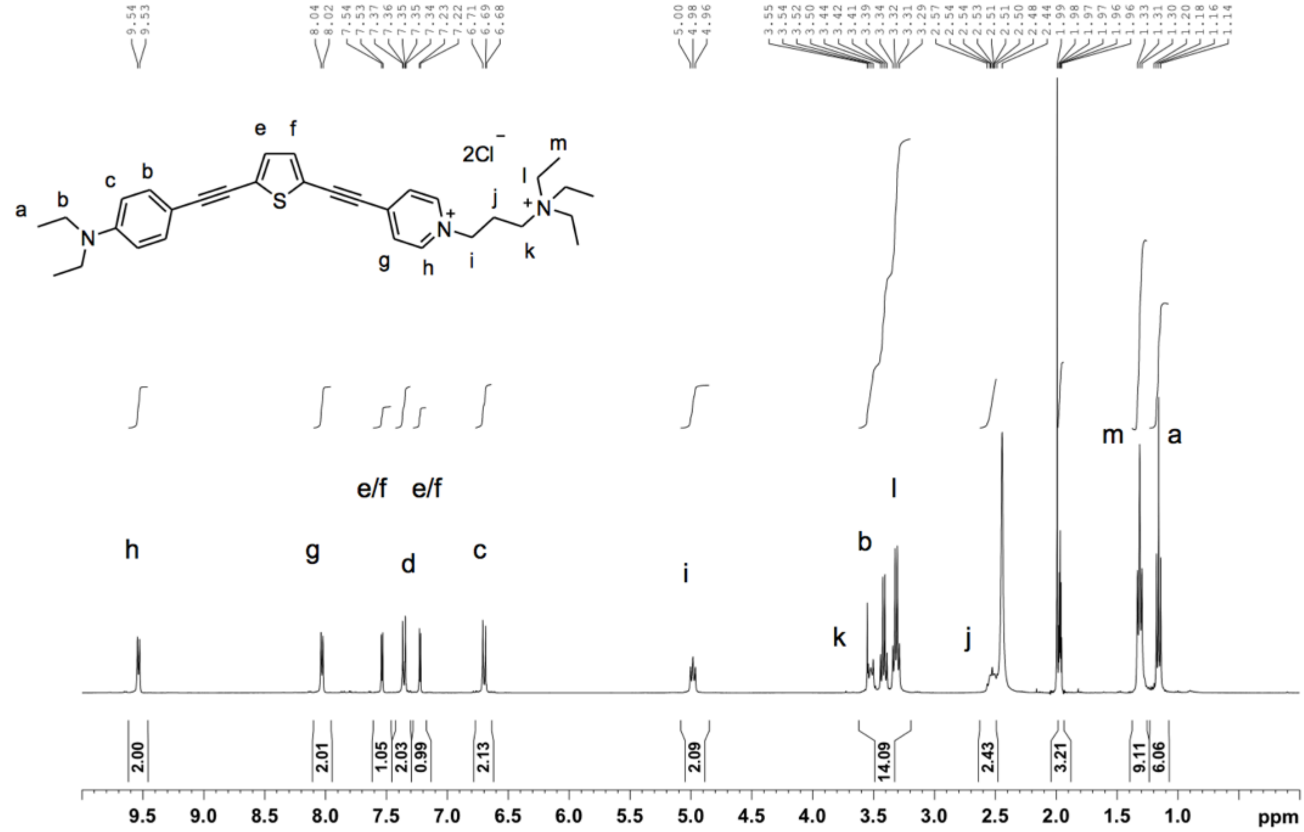

**Fig. S7.** $^1$H NMR spectrum of **2b** (400 MHz, $CD_3CN$).

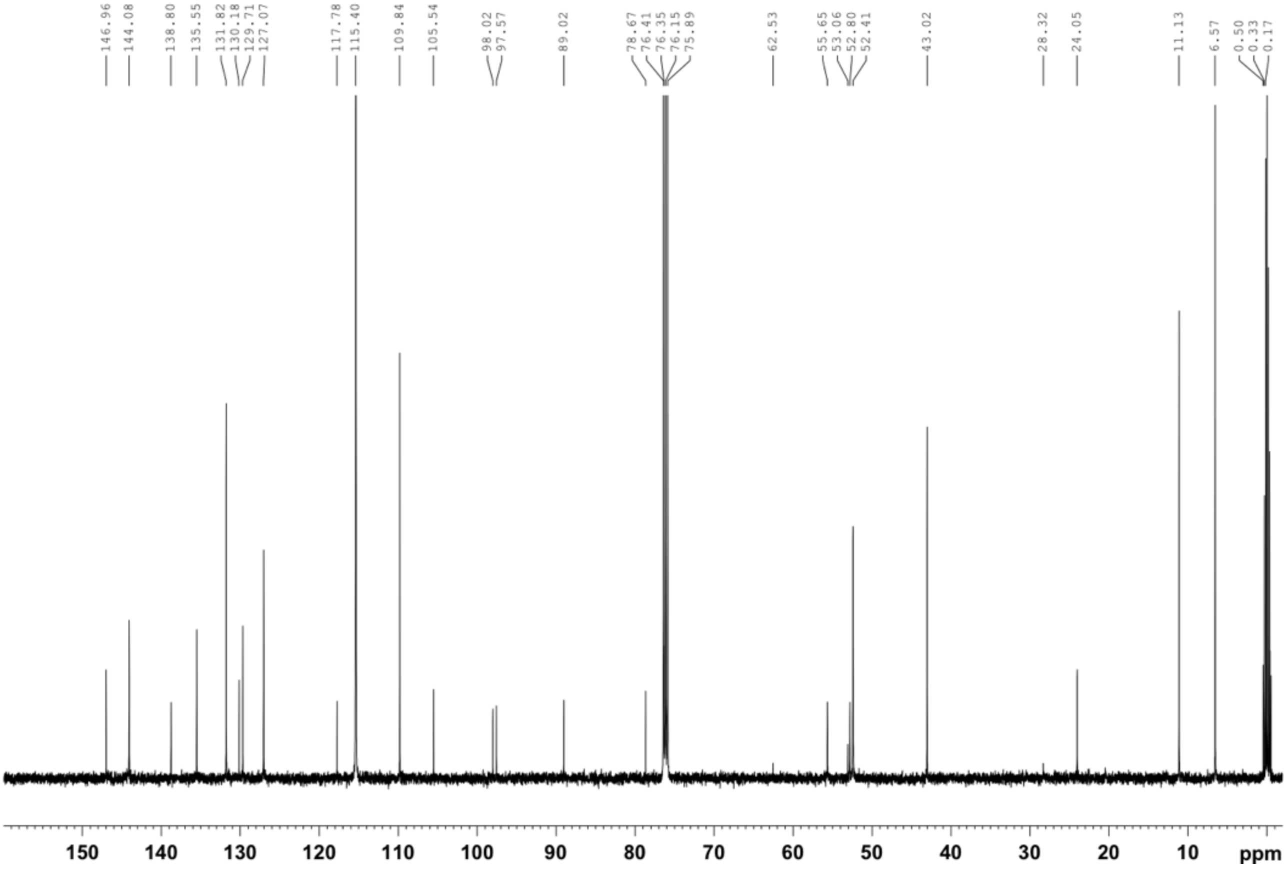

**Fig. S8.** $^{13}$C NMR spectrum of **2b** (100 MHz, $CDCl_3$ + $CD_3CN$).

**Table S1** Photophysical properties of **FM4-64**, **1b** and **2b** in different solvents.

| | $E_T^N$ | $\varepsilon$ | $\lambda_{max}^{abs}$ (nm) | $\lambda_{max}^{em}$ (nm) | $\Phi_{Fl}$ | $\tau$ (ns) | $k_r$ ($s^{-1}$) | $k_{nr}$ ($s^{-1}$) |
|---|---|---|---|---|---|---|---|---|
| **FM4-64** | | | | | | | | |
| $H_2O$ | 1 | 80.1 | 501 | > 850[a] | 0.002[d] | 0.1[d] | | |
| MeOH | 0.762 | 33 | 547 | > 850[a] | 0.02[d] | 0.2 | 1.0E+08 | 4.9E+09 |
| MeCN | 0.46 | 36.64 | 537 | 830 | 0.03[d] | 0.47 | 6.4E+07 | 2.1E+09 |
| DCM | 0.309 | 8.93 | 551 | 793 | 0.21 | 1.0 | 2.1E+08 | 7.9E+08 |
| $CHCl_3$ | 0.259 | 4.81 | 564 | 761 | 0.35 | 1.3 | 2.7E+08 | 5.0E+08 |
| PhMe | 0.099 | 2.38 | 500 | 701 | 0.013[c] | 0.62 | 2.1E+07 | 1.6E+09 |
| **1b** | | | | | | | | |
| $H_2O$ | 1 | 80.1 | 477 | [b] | [b] | [b] | | |
| MeOH | 0.762 | 33 | 555 | > 850[a] | 0.0005[d] | [b] | | |
| MeCN | 0.46 | 36.64 | 545 | 860 | 0.0004[d] | [b] | | |
| DCM | 0.309 | 8.93 | 555 | 824 | 0.04 | 0.57 | 7.0E+07 | 1.7E+09 |
| $CHCl_3$ | 0.259 | 4.81 | 568 | 796 | 0.25 | 1.1 | 2.3E+08 | 6.8E+08 |
| PhMe | 0.099 | 2.38 | 488 | 718 | 0.011[c] | 1.4 | 7.9E+06 | 7.1E+08 |
| **2b** | | | | | | | | |
| $H_2O$ | 1 | 80.1 | 450 | [b] | [b] | [b] | | |
| MeOH | 0.762 | 33 | 487 | [b] | [b] | [b] | | |
| MeCN | 0.46 | 36.64 | 480 | [b] | [b] | [b] | | |
| DCM | 0.309 | 8.93 | 491 | 798 | 0.002 | | | |
| $CHCl_3$ | 0.259 | 4.81 | 506 | 723 | 0.0085 | 0.1[d] | 8.5E+07 | 9.9E+09 |
| PhMe | 0.099 | 2.38 | 463 | 648 | 0.026[c] | 0.66 | 3.9E+07 | 1.5E+09 |

[a] Outside of detectable range. [b] No fluorescence signals detected. [c] Excitation wavelength dependent. [d] Approximate value (lower estimate) due to the spectrum falling outside detectable range.

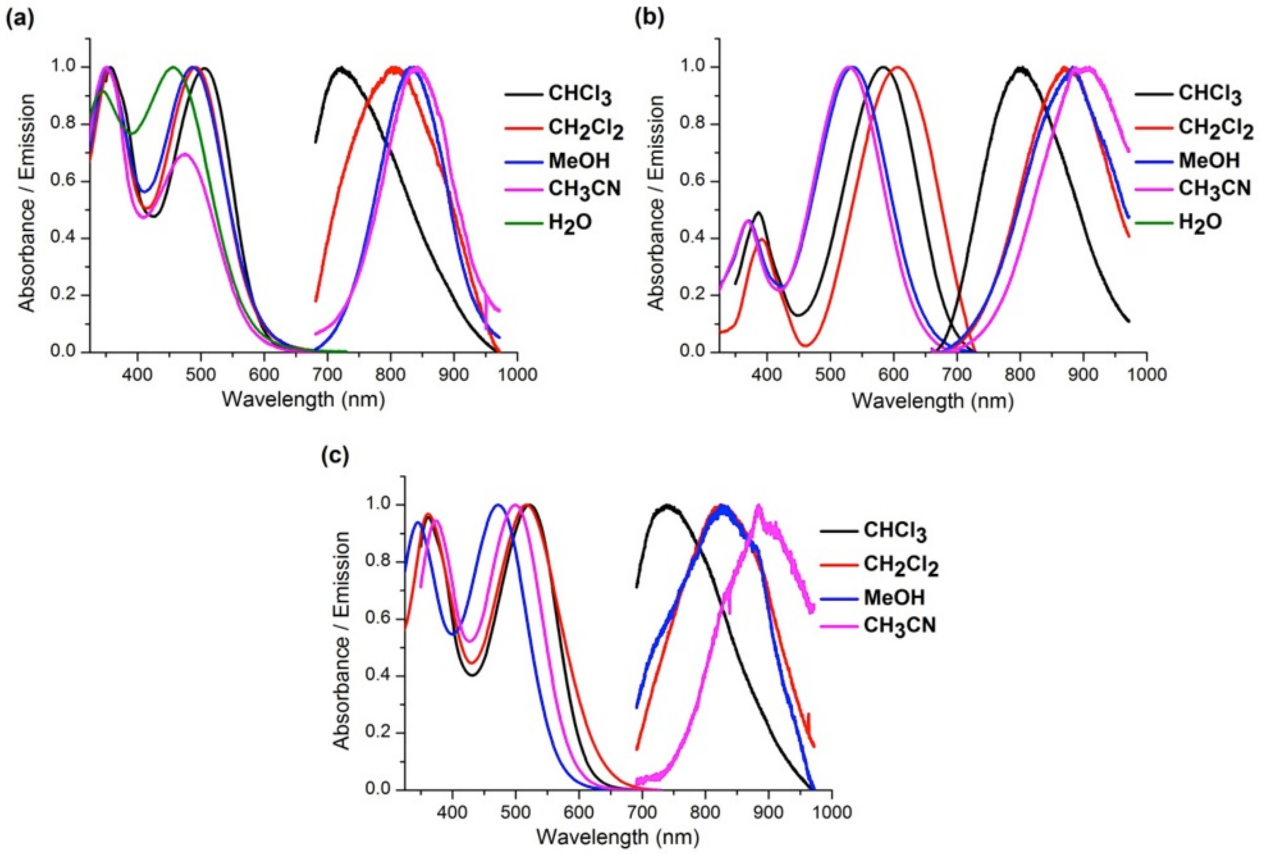

**Fig. S9.** Normalized absorption and emission spectra of **2b** (a), **1a** (b) and **2a** (c) in a variety of solvents with increasing polarity.

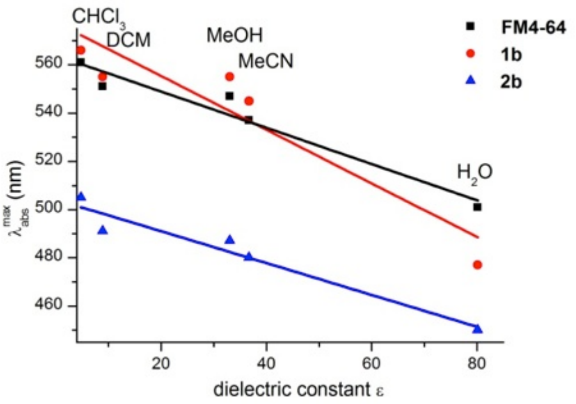

**Fig. S10.** Plot of absorption maxima of **FM4-64** (black squares), **1b** (red dots) and **2b** (blue triangles) against the solvent dielectric constants. Note, toluene data are not included due to aggregation as explained in the text.

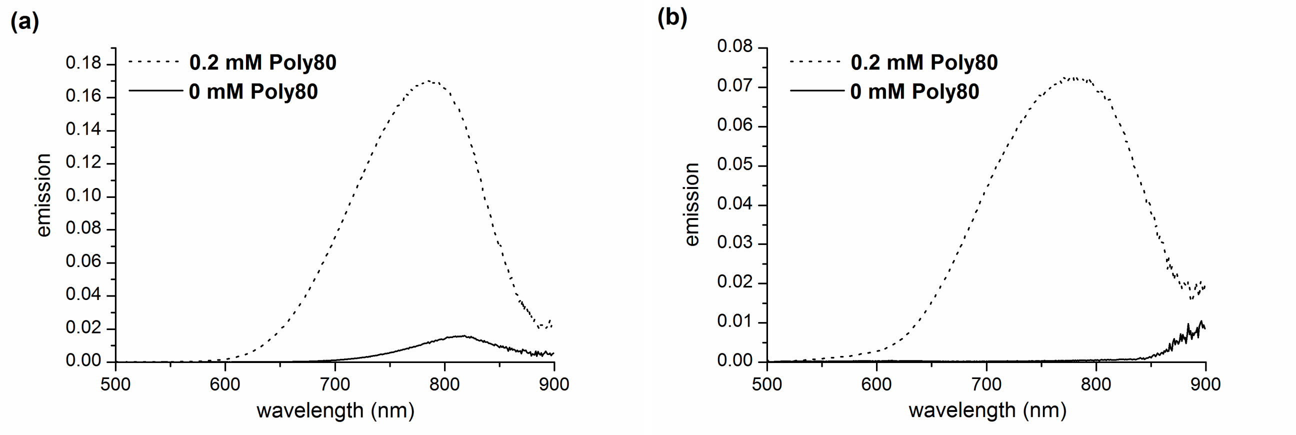

**Fig. S11.** Fluorescence spectra of **FM4-64** (a) and **1b** (b) in water (solid lines) and micelles (dotted lines). Dye concentration was 1 µM in both solvents. Concentration of surfactant (polysorbate-80, 0.2 mM in water) was above the critical micelle concentration.

## 3) Hyper-Rayleigh Scattering

The molecular first hyperpolarizabilities were characterized through hyper-Rayleigh scattering (HRS) experiments,[6,7] using a femtosecond pulsed titanium sapphire laser (Spectra-Physics, model Millennia X to pump the model Tsunami, with a lock-to-clock system to provide an 80 MHz pulsed output) at a fundamental wavelength of 800 nm in combination with a low-frequency lock-in amplifier and a signal generator for analyzing and correcting for any multiphoton contribution to the HRS signal at the second harmonic wavelength of 400 nm. Details can be found elsewhere.[8,9] Using the 90° geometry, the measured HRS hyperpolarizabililty can be related to the diagonal component of the molecular first hyperpolarizability:

$$\langle \beta_{\mathrm{HRS}}^2 \rangle \approx \frac{6}{35} \beta_{\mathrm{zzz}}^2. \tag{S1}$$

Equation (S1) is valid for molecules with approximate $C_{\infty v}$ symmetry, such as the chromophores considered in this study, where the optical response is clearly dominated by a single and succinctly defined charge-transfer absorption band along the molecular dipolar *z*-axis. Therefore the HRS response is dominated by the contribution of the single major diagonal component of the first hyperpolarizability $\beta_{zzz}$. The well-separated absorption band originating from the transfer between HOMO and LUMO also justifies the use of the two-level model[10] to derive static $\beta_{zzz,0}$ values. The demodulation technique revealed that there was no fluorescence contribution to the signal at 400 nm, as the apparent hyperpolarizability was constant as a function of modulation frequency. Therefore, the fluorescence-free hyperpolarizability could be determined accurately and precisely, as the average value over the different modulation frequencies.

## 4) Dark Toxicity and Phototoxicity Experimental Procedures

**Cell Culturing:** Media (DMEM, Sigma, 10% FBS, 1% PS, 1% LG) was removed from confluent cells (HeLa) in culture. After washing the cell flask with PBS (25 mL), the cells were removed from the surface of the flask with a solution of trypsin (0.25% in EDTA, 5 mL) and incubated for 1 min until the cells were seen to be detached under magnification. Cells to be subcultured were then resuspended in fresh media (25 mL).

**Dark Toxicity.** The HeLa cells were seeded in flat 96-well plates (Fisher) at a density of 1,000 cells per well in 100 µL of culture media. The cells were then allowed to settle down and adhere to the wells for 2 h before the media was replaced with the solution of a dye at eight different concentrations (0.5, 1.0, 2.5, 5.0, 10, 25, 50, and 100 µM), which were diluted from a 10 mM stock in DMSO with media containing 1% DMSO. The microplates were shielded from light during and after incubation. After 3 h incubation, the dye solution was removed and the cells were washed three times with 100 µL of media and further incubated in 100 µL of fresh media for 2 days. After that, the cell viability was determined by adding 20 µL of a proliferation assay (CellTiter 96R, Promega) into each well of the microplates and incubating them for further 2 hours before the absorbance of the solution was checked using a microplate reader (Benchmark Plus Microplate Spectrophotometer, Bio-Rad) at 490 nm. An average background absorbance reading of the media was recorded and subtracted from the average absorbance of each replicate group, before further data manipulation. Each experimental condition consisted of 6 replicates and the experiment was repeated at least twice to ensure that the results were reproducible.

**Phototoxicity**. Similar cell preparation as for the dark toxicity experiments was employed; nonetheless, only two concentrations of each dye were tested for phototoxicity as a function of light dose. After 3 h incubation with the dye solution, the microplates were placed on the light box, which contained six green LEDs ($\lambda_{max}$ = 525 nm, FWHM = 32 nm, 0.85 mW, Dotlight, Germany) in every other column. Each LED was placed directly under one of the wells in the sample plate to ensure that the samples would receive the same light intensity. The sample and spacer microplates had black walls with a transparent base and the light was directed to only the sample well, thus each well was optically isolated. Moreover, the plates were sealed with a black lid and handled in low light conditions to prevent ambient or scattered excitation light falling on the samples. The wells required light exposure were irradiated with green LEDs for 10, 20, 30 and 40 min before being washed three times with 100 µL of media and further incubated in 100 µL of fresh media for 2 days. After that, cell viability was determined using the same procedure used in dark toxicity experiments.

## 5) Dark Toxicity Data

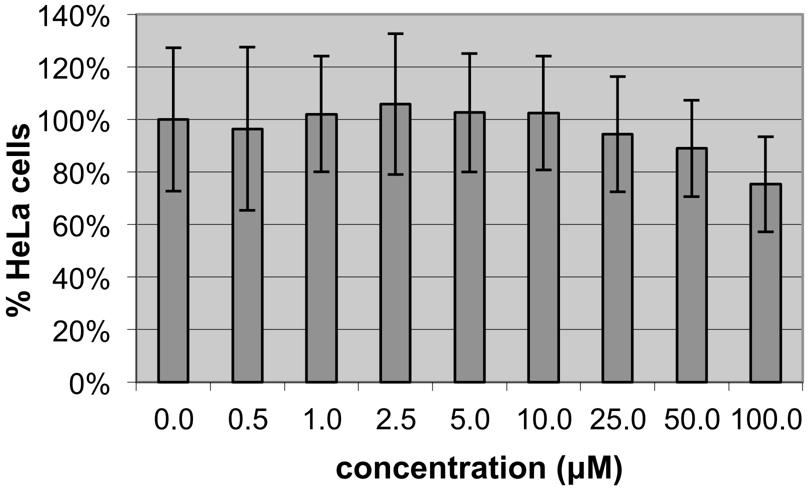

**FM4-64**

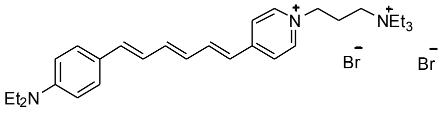

Chemical Formula: $C_{30}H_{45}Br_2N_3$
Molecular Weight: 607.5064

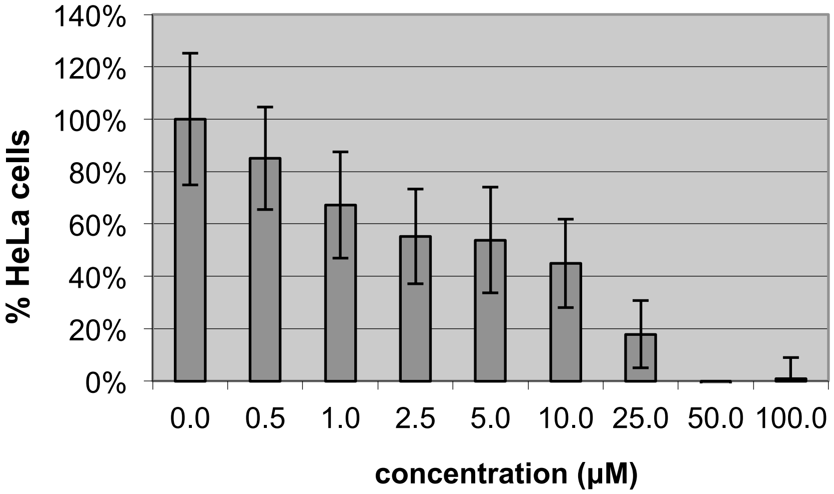

**1a**

LC50 = 8.3 µM

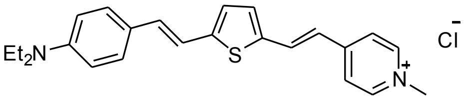

Chemical Formula: $C_{24}H_{27}ClN_2S$
Molecular Weight: 411.0026

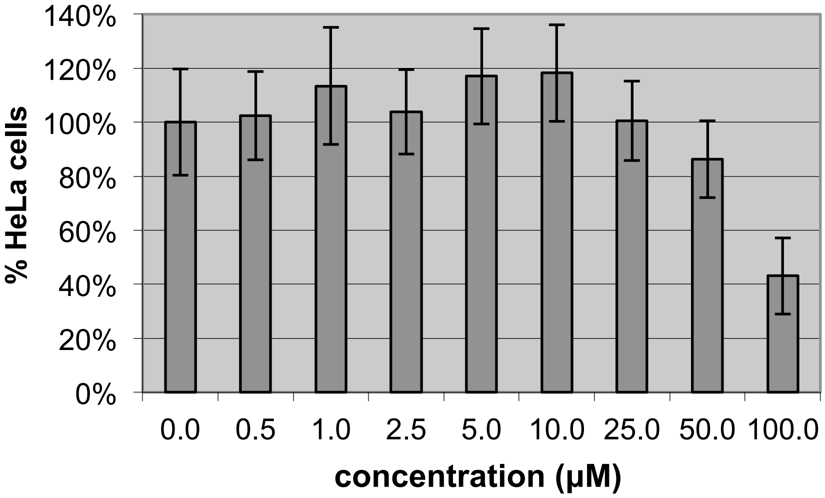

**1b**

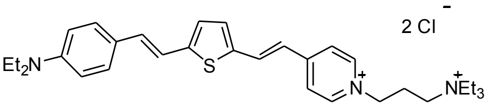

Chemical Formula: $C_{32}H_{45}Cl_2N_3S$
Molecular Weight: 574.6908

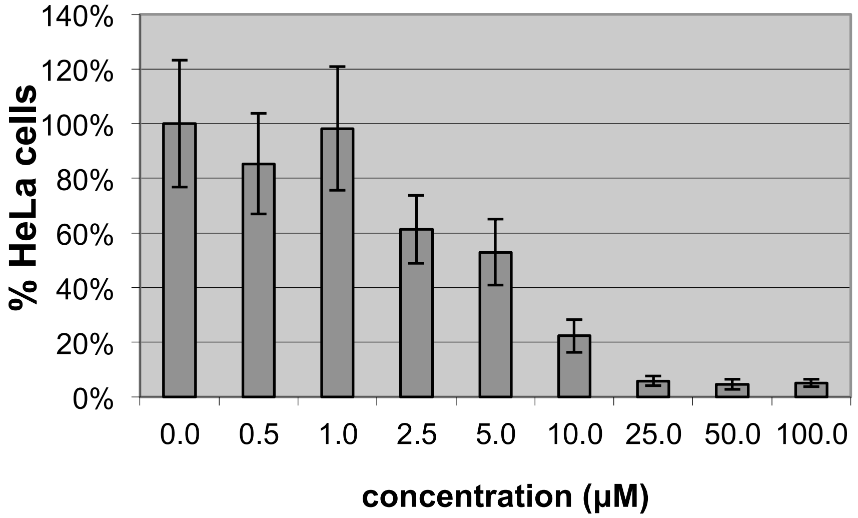

**2a**

LC50 = 4.6 µM

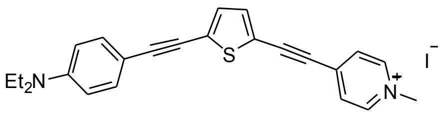

Chemical Formula: $C_{24}H_{23}IN_2S$
Molecular Weight: 498.4223

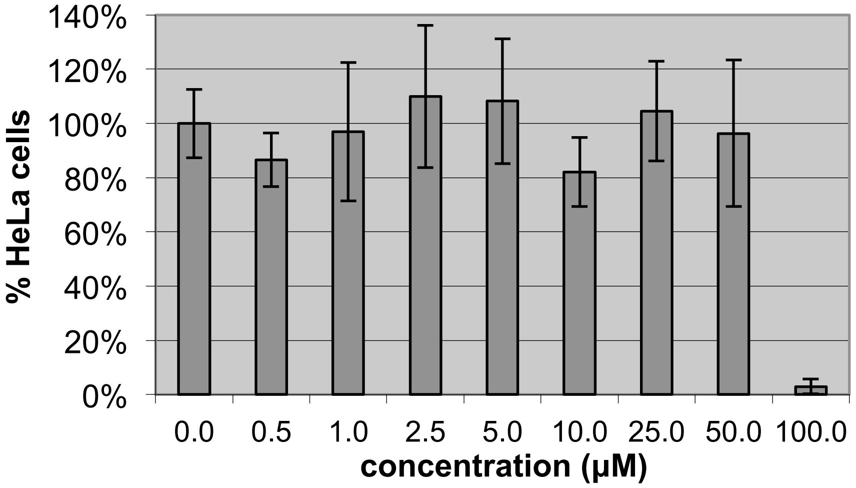

**2b**

LC50 = 92 µM

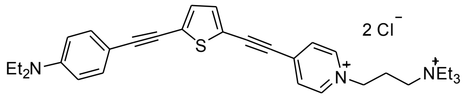

Chemical Formula: $C_{32}H_{41}Cl_2N_3S^{2+}$
Molecular Weight: 570.6579

## 6) Phototoxicity Data

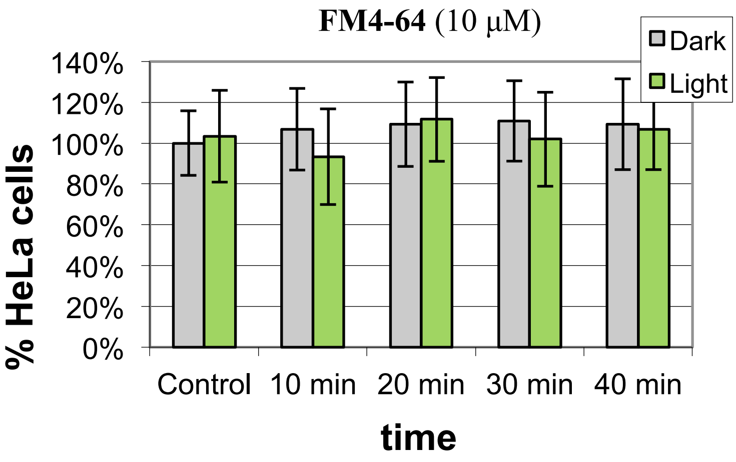

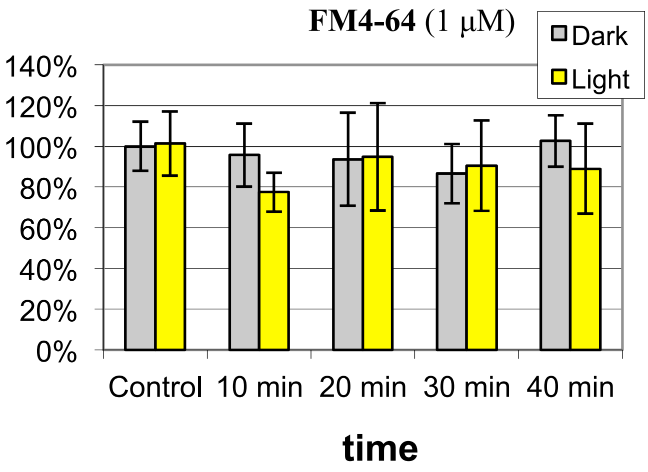

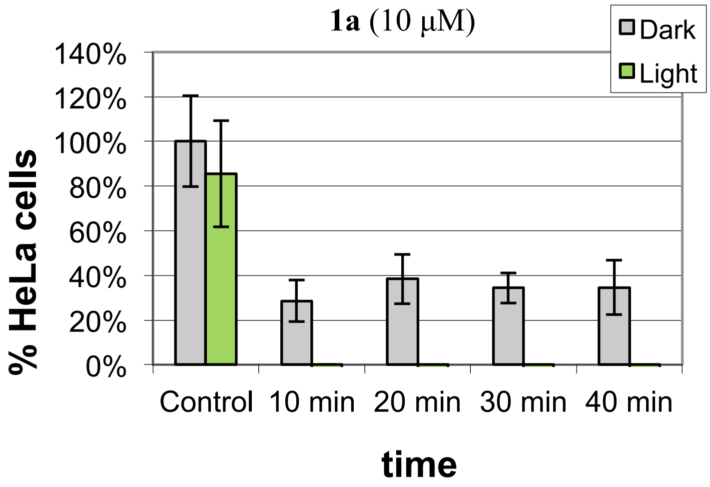

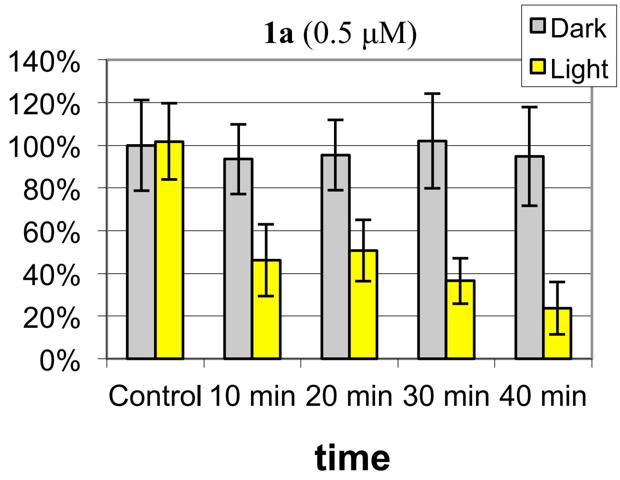

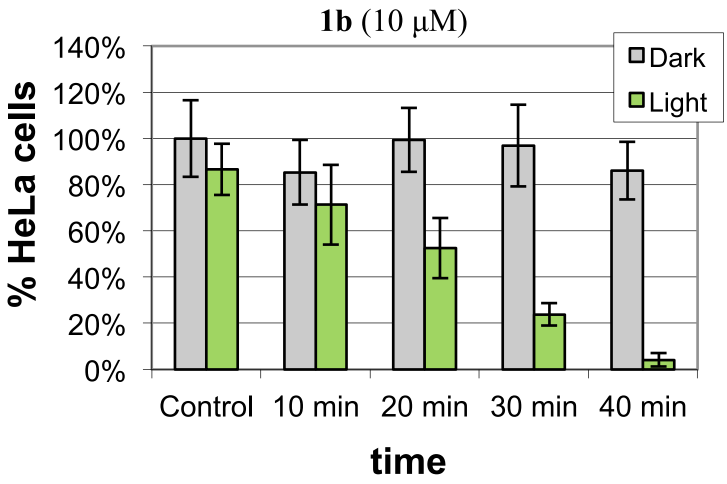

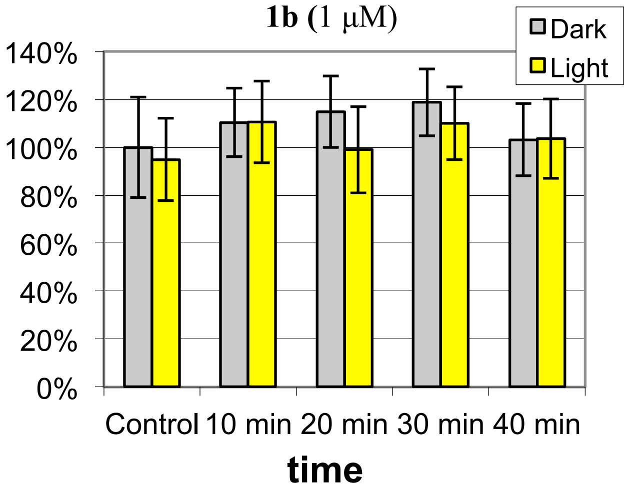

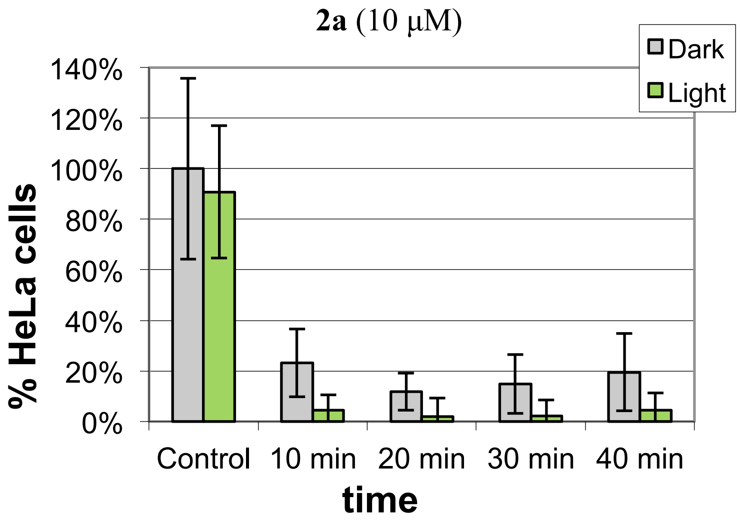

**2a** (10 µM)

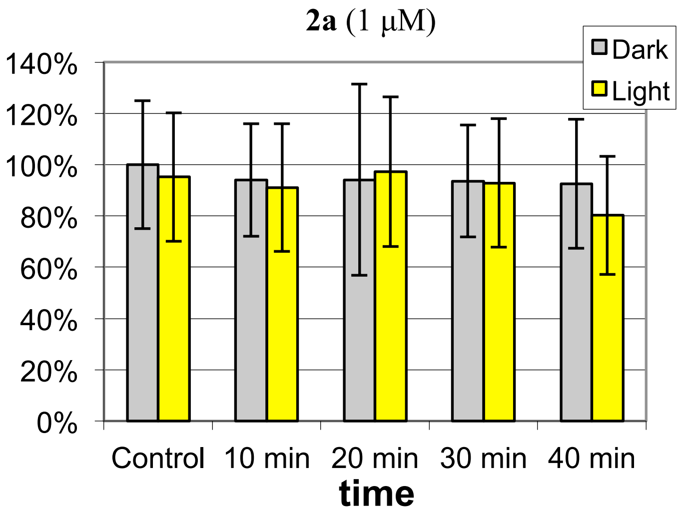

**2a** (1 µM)

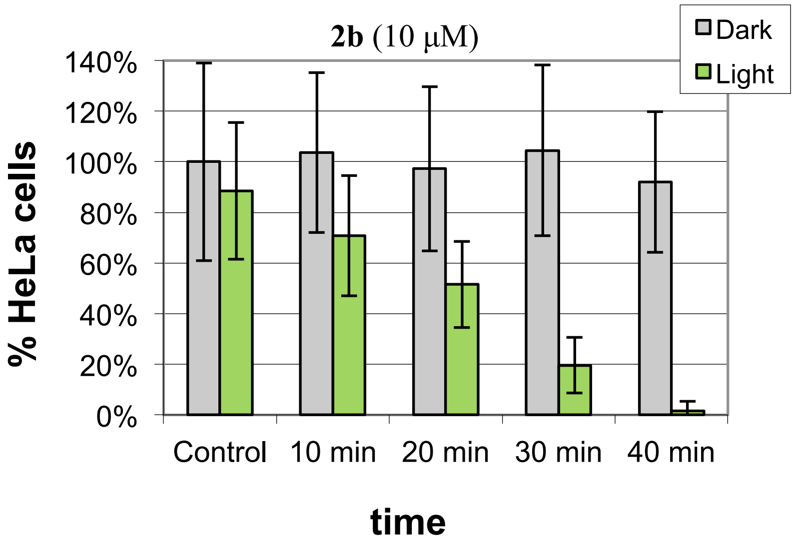

**2b** (10 µM)

## 7) Fluorescence Imaging

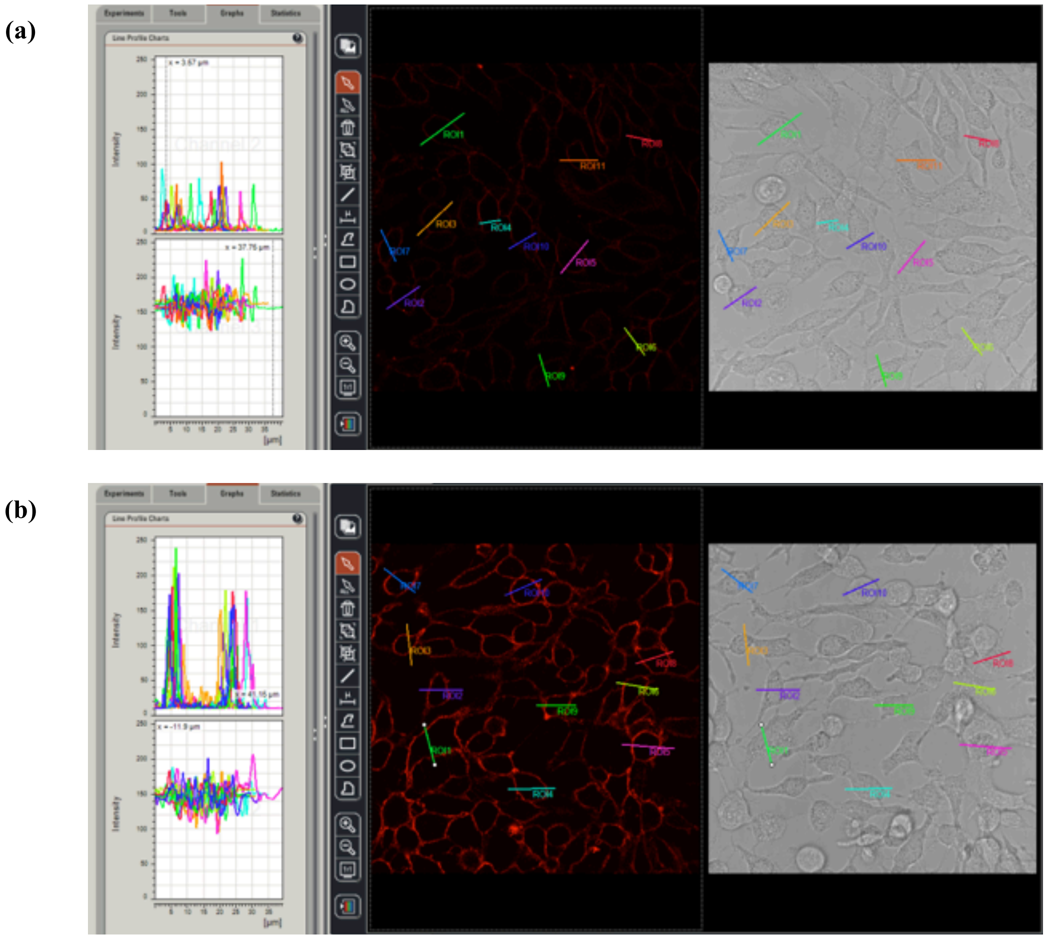

**Fig. S12.** Direct fluorescent intensity comparison between **FM4-64** (a) and **1b** (b) in live cells as demonstrated by the screen views of Leica LAS AF Lite Software. Detector settings and acquisition conditions for both images were identical. The lower intensity of the fluorescence image in (a) is clear to see. Furthermore, for direct quantitative comparison multiple cross sections of cells in fluorescence images were taken (shown by the colored bars in the images). These data are summarized on the top left in each Figure. Fluorescence channel intensities are vastly different for **FM4-64** and **1b** with average intensity of 70 a.u. for **FM4-64** in cells (a) and of 200 a.u. for **1b** (b).

**Cellular Uptake.** The cellular uptake of the new family of thiothene-based dyes is extremely fast when delivered in a standard DMEM medium (less than 1 min, for internalization and cytoplasmic organelle staining). However when the procedure to stop endocytosis is employed (4 °C incubation, $Mg^{2+}$ and $Ca^{2+}$ free medium) internalization does not occur for **1b** or **2b** up to 12 h. The rate of cellular uptake for these dyes in $Mg^{2+}$ and $Ca^{2+}$ free medium at 4 °C, compared to **FM4-64** (all at 10 µM concentration) is shown in Figure S13. The maximum intensity in the plasma membrane of SK-OV-3 cells is achieved in approximately 2–5 min of incubation (**1b** 5× brighter than **FM4-64** and **2b** 2× brighter than **FM4-64**). It could be seen that **2b** displays irradiation-induced internalization at times longer than 15 min, causing internal organelle staining and resulting in phototoxicity.

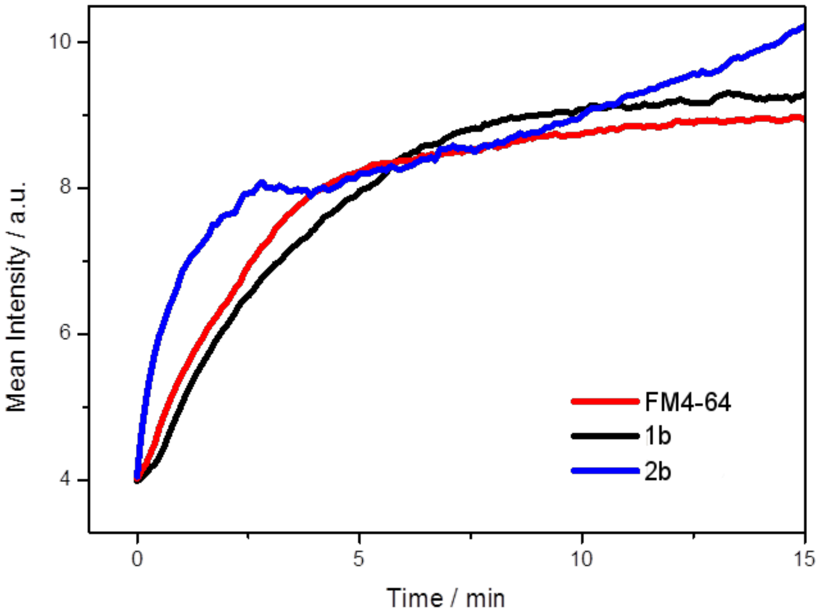

**Fig. S13.** Normalized cellular uptake kinetic plot recorded by monitoring a mean fluorescence signal from the confluent layer of cells upon addition of the $Mg^{2+}$ and $Ca^{2+}$ free medium at 4 °C containing 2.5 µM of each dye. The interval between each recorded image frame was 3 s. Normalization factors: **FM4-64** (×1); **1b** (×0.2); **2b** (×0.5).

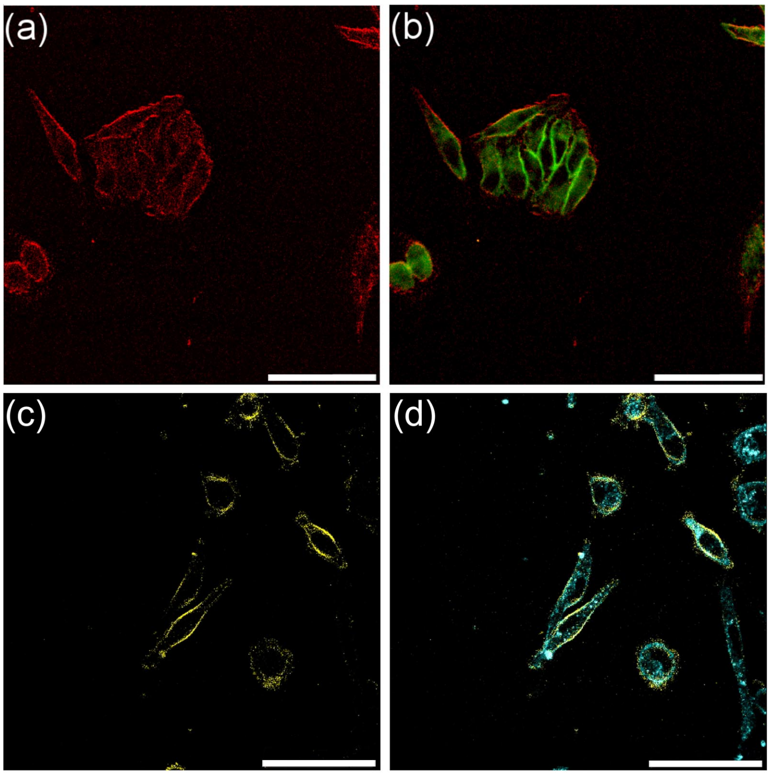

**Fig. S14.** Scanning confocal multiphoton microscopy images of HeLa cells (a, b) and MDA-231 cells (c, d) stained with **2b** (a, b) or **1b** (c, d) showing SHG (a, c) and SHG overlaid with fluorescence (b, d). All scale bars are 75 µm. Note that the image (c) for **1b** is recorded with identical settings and magnification as for **FM4-64** (main text, Figure 7D), however, the signal is significantly brighter for **1b**, indicating that it is a more efficient SHG probe.

## 8) Voltage-Sensitive SHG and Fluorescence

To probe the voltage-sensitivity of **FM4-64**, **1b** and **2b** in the SHG and two-photon excited fluorescence channels, hemispherical lipid bilayers (HLBs) used as artificial membrane models. The exterior of the membranes was stained with dye and imaged using the methods and optical setup described in Ref. [11]. A series of linescans across the membrane was acquired as the HLB was subjected to a variable command voltage. Pixel intensities from each linescan were averaged into single data points, and after correcting for photobleaching and background drift, Gaussian noise reduction was performed. The resulting waveforms were used to calculate the sensitivity of the dye to electric field, expressed as a fractional change of signal intensity relative to the mean recorded signal per 100 mV. The sensitivity of a dye is the slope of the least-squares-fitted straight line through the origin, as seen in Figure S18. The data points in Figure S17 are averaged samples of waveforms, such as those depicted in Figures S16–S17, taken from the interval 360–380 ms after each voltage step. Data for **FM4-64** were calculated based on 3 datasets; 4 datasets were used for **2b**, and **1b** results are reported based on two (SHG) and three (TPEF) datasets. The sensitivities of the dyes to voltage are provided in Table S2. Uncertainties are reported as standard errors.

**Table S2** Relative sensitivities of **FM4-64**, **1b** and **2b**.

| | *SHG* *sensitivity per 100 mV* | *TPEF* *sensitivity per 100 mV* |
|---|---|---|
| **FM4-64** | –5.3% ± 0.5% | –3.0% ± 0.5% |
| **1b** | 0.67% ± 0.06% | –7.1% ± 1.3% |
| **2b** | insensitive | insensitive |

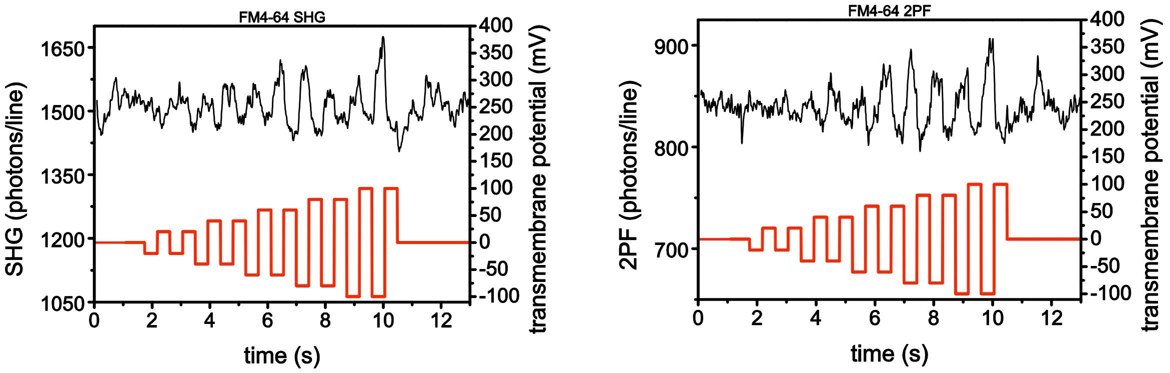

**Fig. S15.** Waveforms showing the the optical response (black curves) of **FM4-64** with changes of the command voltage (red curve)

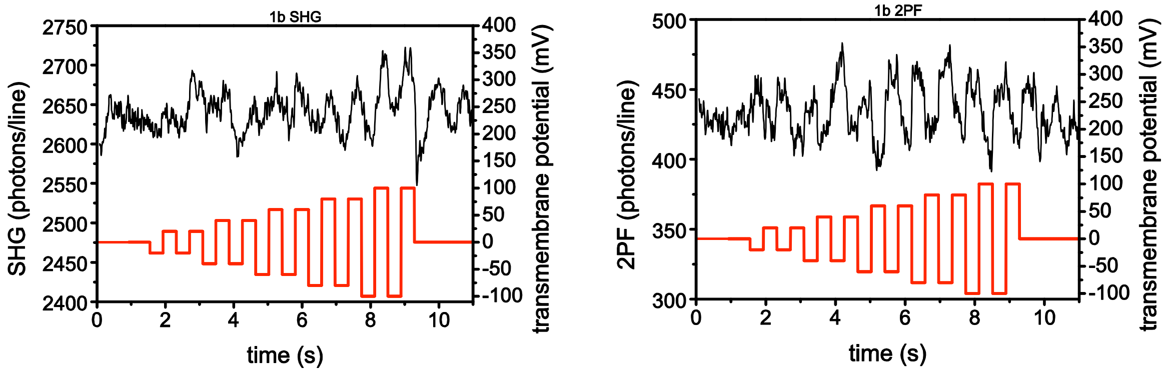

**Fig. S16.** Waveforms showing the the optical response (black curves) of **1b** with changes of the command voltage (red curve)

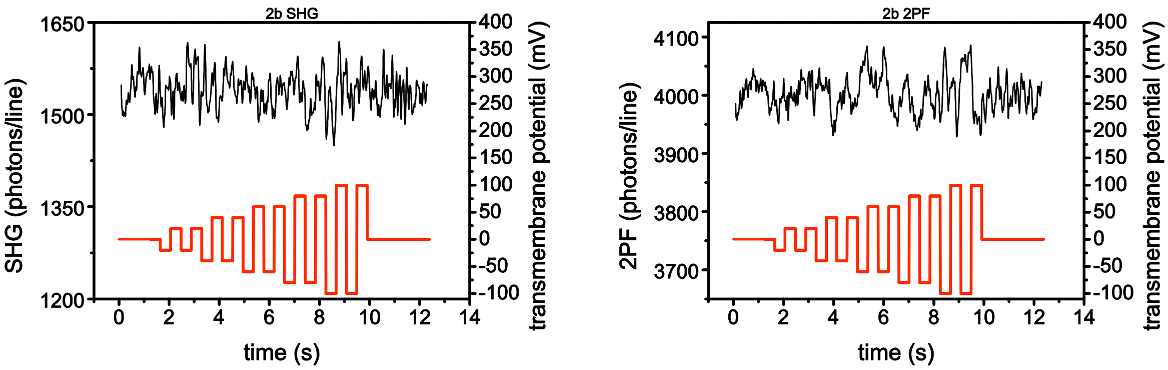

**Fig. S17.** Waveforms showing the the optical response (black curves) of **2b** with changes of the command voltage (red curve)

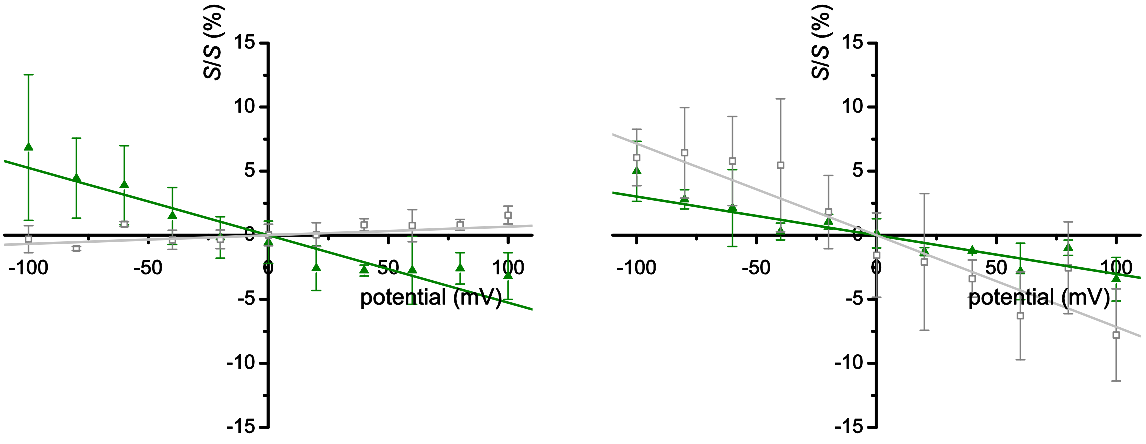

**Fig. S18.** Sensitivity plot showing the relative change in avarage SHG (left) and TPEF (right) response of **FM4-64** (green) and **1b** (grey) to the individual command voltage step. Dye **2b** proved to be unresponsive.

## 9) References

1 J. P. Wuskell, D. Boudreau, M.-d. Wei, L. Jin, R. Engl, R. Chebolu, A. Bullen, K. D. Hoffacker, J. Kerimo, L. B. Cohen, M. R. Zochowski and L. M. Loew, *J. Neurosci. Methods,* 2006, **151**, 200.

2 M. J. Patrick, L. A. Ernst, A. S. Waggoner, D. Thai, D. Tai and G. Salama, *Org. Biomol. Chem.,* 2007, **5**, 3347.

3 W. S. Jeon, E. Kim, Y. H. Ko, I. Hwang, J. W. Lee, S.-Y. Kim, H.-J. Kim and K. Kim, *Angew. Chem. Int. Ed.,* 2005, **44**, 87.

4 P. Yan, A. Xie, M. Wei and L. M. Loew, *J. Org. Chem.,* 2008, **73**, 6587.

5 R. Wu, J. S. Schumm, D. L. Pearson and J. M. Tour, *J. Org. Chem.,* 1996, **61**, 6906.

6 K. Clays and A. Persoons, *Phys. Rev. Lett.*, 1991, **66**, 2980.

7 K. Clays and A. Persoons, *Rev. Sci. Instrum.*, 1992, **63**, 3285.

8 G. Olbrechts, R. Strobbe, K. Clays and A. Persoons, *Rev. Sci. Instrum.*, 1998, **69**, 2233.

9 K. Clays, K. Wostyn, K. Binnemans and A. Persoons, *Rev. Sci. Instrum.*, 2001, **72**, 3215.

10 J. L. Oudar and D. S. Chemla, *J. Chem. Phys*., 1977, **66**, 2664.

11 J. E. Reeve, A. D. Corbett, I. Boczarow, W. Kaluza, W. Barford, H. Bayley, T. Wilson and H. L. Anderson, *Angew. Chem. Int. Ed.*, 2013, **52**, 9044.